Applied Ergonomics 100 (2022) 103663

Contents lists available at ScienceDirect

Applied Ergonomics

journal homepage: www.elsevier.com/locate/apergo

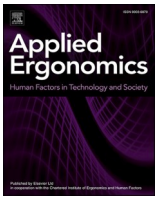

In contrast to slip-resistant shoes, fluid drainage capacity explains friction performance across shoes that are not slip-resistant

Emily E. Meehan [a], Natasa Vidic [b], Kurt E. Beschorner [a,*]

[a] Bioengineering Department, University of Pittsburgh, 3700 O'Hara St. #302, Pittsburgh, PA, 15261, USA
[b] Industrial Engineering Department, University of Pittsburgh, 3700 O'Hara St. #1007, Pittsburgh, PA, 15261, USA

ARTICLE INFO

Keywords:
Slips
Trips
And falls
Coefficient of friction
Footwear

ABSTRACT

Slip and fall injuries can be prevented through footwear with good friction performance. The factors that contribute to friction in non-slip-resistant (NSR) shoes are not well understood. The purpose of this study was to determine whether predictive models for slip-resistant (SR) shoes also apply to NSR shoes. This study also quantified the contributions of under-shoe fluid drainage to friction in NSR shoes. The coefficient of friction (ACOF) and under-shoe fluid pressures of fifteen NSR shoes were measured. A previously developed ACOF prediction model based on measurable outsole features was applied to the NSR shoes. The previously developed model did not apply well (in trends, as indicated by interaction effects involving SR/NSR classification, or in magnitude, $p < 0.001$) to NSR shoes. Instead, an increase in the fluid pressures were associated with a reduction in ACOF ($p < 0.001$). This study demonstrates that fluid pressures dominate performance in NSR shoes in contrast to SR shoes.

1. Introduction

Slips and falls represent a concerning problem in both the home and the workplace. In 2019, slips, trips and falls accounted for over 240,000 nonfatal occupational injuries (Bureau of Labor Statistics, 2020). Unintentional falls also led to over 3 million emergency department visits among persons aged 15–64 years (National Center for Injury Prevention and Control, 2020). These accidents have important financial consequences. In 2013, emergency-department treated nonfatal fall injuries accounted for about 37% of all costs (~$169 billion) related to medical expenses and lost wages (Florence et al., 2015). Slippery conditions contribute to 40–50% of occupational fall injuries to the same level (Courtney et al., 2001; U.S. Department of Labor- Bureau of Labor Statistics, 2020). Because slipping is an important cause of falling, understanding and reducing causes of slipping is an important priority.

Slips occur when there is not enough friction between the shoe and floor to maintain the dynamics of walking (Hanson et al., 1999; Iraqi et al., 2018a). Available coefficient of friction, ACOF, is a common measure of the friction between the outsole of the shoe and the floor. The outsole of the shoe is important because it forms the contact interface with the floor and generates the friction required during stance. Higher friction performance can predict a reduction in slip events (Bagheri et al., 2021; Burnfield and Powers, 2006; Iraqi et al., 2018a). The ACOF is often measured with a shoe-floor tribometer such as the Portable Slip Stimulator (Aschan et al., 2005). The ACOF is an integrative measure across multiple friction and lubrication phenomena (Chang et al., 2001b; Grönqvist, 1995; Moghaddam et al., 2018; Sundaram et al., 2020) and is dependent on the shoe surface, the flooring counter-surface, and any liquid contaminant within the interface (Chen et al., 2015; Jones et al., 2018; Li and Chen, 2005). All these factors contribute to the resulting friction especially the viscosity of the liquid and the topography of the flooring (Chang, 1998; Chang et al., 2001a, 2004; Moore et al., 2012). Footwear design also influences friction performance on icy surfaces (Bagheri et al., 2019a, 2019b, 2019c) although the friction mechanisms (Rizvi et al., 2015) and subsequently the preferable footwear design features (Bagheri et al., 2019a, 2019b, 2019c; Roshan Fekr et al., 2021) are different between icy and liquid-contaminated conditions. Popular footwear has been shown to have poor friction performance in icy conditions (Bagheri et al., 2019b, 2019c). The present study will determine the factors contributing to oily friction performance for popular footwear.

The ACOF varies across shoes and shoe design features, such as its

ACOF, Coefficient of friction; NSR, Non-slip-resistant; SR, Slip-resistant

* Corresponding author.
E-mail address: beschorn@pitt.edu (K.E. Beschorner).

https://doi.org/10.1016/j.apergo.2021.103663
Received 24 August 2021; Received in revised form 12 November 2021; Accepted 29 November 2021
Available online 8 December 2021

geometry and material (Yamaguchi et al., 2017, 2018). A previous study on shoes labeled as slip-resistant (SR) found that tread surface area, heel shape, and hardness (while controlling for flooring) predict 87% of the variation in ACOF under oily conditions (Iraqi et al., 2020). However, it is unclear whether this finding extends to shoes that are non-slip resistant (NSR). Designers of SR shoes make intentional design choices like using small tread lugs patterned across the shoe surface (Kubis and Randesi, 2013) to promote drainage and good friction via high tread surface area in the presence of oil and other floor contaminants (Beschorner et al., 2020; Hemler et al., 2020; Moghaddam and Beschorner, 2018; Yamaguchi et al., 2017). Thus, their design likely deviates from other shoe designs, which may be placing more priority to comfort, aesthetics, and cost. Indeed, slip resistant (SR) shoes worn by restaurant workers resulted in a 54% reduction in reported slips compared to their NSR counterparts (Verma et al., 2011). Easing the burden of fall injuries requires strategies that enhance friction performance of both SR shoes and NSR shoes. However, it is not well understood whether the tread features that predict ACOF for SR shoes also apply to NSR shoes.

Research has shown that shoes can improve friction performance by making certain design choices. SR shoes with lower hardness have shown improved ACOF (Iraqi et al., 2020; Jones et al., 2018). Geometry of the tread features, including their cross-sectional size and height, also influence friction by altering the size of the contact region when friction-induced bending is applied (Hale et al., 2021; Yamaguchi et al., 2017). Specifically, SR shoes can improve friction performance by increasing the tread surface area in the posterior outsole, which is positively correlated with ACOF (Iraqi et al., 2020; Jones et al., 2018). Tread channel pattern (including depth and width) may potentially influence the ACOF although evidence is mixed (Blanchette and Powers, 2015; Li and Chen, 2004; Yamaguchi et al., 2017). The tread pattern affects hydrodynamic pressure under the shoe; fluid without an escape pathway gets pressurized and decreases the ACOF (Strandberg, 1985; Tisserand, 1985). SR shoes typically have sufficient tread channels to minimize fluid pressurization in their new condition (Hemler et al., 2019). In contrast, the design of NSR shoes varies widely in material and tread pattern. Furthermore, fluid pressures have been observed for certain designs of NSR shoes (Iraqi, 2013). Given the difference between the design of SR and NSR shoes, the parameters that can predict ACOF for SR shoes may not predict ACOF for NSR shoes.

The main mechanisms that affect the shoe-floor-liquid contaminant ACOF are hysteresis friction and hydrodynamic pressure. Hysteresis friction results from the loss of viscoelastic energy that occurs when the softer material of the shoe outsole interacts with the hard surface asperities of the floor (Iraqi et al., 2020; Moghaddam et al., 2015; Persson, 2001). Hysteresis friction contributes more to the overall friction than adhesion friction when the surface is lubricated (Strobel et al., 2012). Since high tread surface area, beveled shoes, and lower hardness contribute to increased hysteresis friction in oily conditions for SR shoes, we hypothesize that these factors may similarly influence hysteresis friction for NSR shoes. The other mechanism that could affect ACOF in NSR shoes is hydrodynamic pressure. Hydrodynamic lubrication occurs in a slipping scenario as the shoe and the floor are separated by a thin layer of fluid – the contaminant (Beschorner et al., 2014). The increase in hydrodynamic lubrication results because the fluid contaminant becomes pressurized, so the shoe sole and floor separate, which will decrease the ACOF (Beschorner and Singh, 2012; Hamrock et al., 2004; Hemler et al., 2020; Sundaram et al., 2020). A major difference between SR and NSR shoes is the tread pattern. Many NSR shoes have an enclosed tread pattern where borders around the tread features inhibit fluid drainage (Iraqi, 2013). Without tread channels that allow for an escape of fluid, the risk of slipping increases (Beschorner et al., 2014; Strandberg, 1985; Tisserand, 1985). Because of preliminary evidence that NSR shoes sometimes have poor drainage patterns compared to SR shoes (Iraqi, 2013; Sundaram et al., 2020), we hypothesize that fluid pressure in NSR shoes may be a predictor of their frictional performance.

The purpose of this study is to quantify whether a predictive regression model developed for SR shoes (based on the tread surface area, shoe beveling, and hardness) (Iraqi et al., 2020) similarly applies to NSR shoes. We hypothesize that this model will predict COF for NSR shoes similar to the SR shoe predictions. In addition, we also predict that fluid pressure will contribute to shoe-floor friction.

2. Materials and methods

To achieve the purpose of this study, ACOF and shoe tread parameter data (tread surface area, hardness, and heel beveling) from a previous study on SR shoes (Iraqi et al., 2020) was combined with newly collected data on NSR shoes. Data collected for NSR shoes included ACOF, shoe tread parameter data (tread surface area, shoe beveling, and hardness), and under-shoe fluid pressures.

2.1. Selection of shoes

A total of 15 common NSR shoes were selected (see Table 1). These shoes were from three different styles: athletic (n = 5), dress (n = 5), and comfort (n = 5). The shoes were selected from five major online footwear retailers (annual revenue for 2019): Amazon and its subsidiary Zappos, ($3.9 billion), Macy's ($940 million), Foot Locker ($680 million), and ShoeBuy ($510 million). Online retail sites were used instead of physical retail stores because online sites commonly advertise the shoes that are the most popular. These vendors were chosen because they collectively accounted for 40% of the online shoe retail market. More NSR shoes were chosen from Amazon (and its subsidiary Zappos) than the other vendors as these companies hold a higher market share. Shoes were selected from October 2018 to January 2019 according to each website's best-seller list. The list of selected shoes, vendors, style, and gender label is presented in Table 1. High heel shoes were excluded from this study since they influence gait patterns (Schaefer and Lindenberger, 2013) and the friction testing methods were validated for slips in non-heeled shoes (Iraqi et al., 2018a).

2.2. Collection of data using lab equipment

ACOF and peak under-shoe fluid pressure were measured, while a mechanical device simulated the dynamics of slipping. The slip tester was modeled after the portable slip simulator (Aschan et al., 2005; Iraqi et al., 2018a). The slip tester has three vertical motors and one horizontal motor. These motors were responsible for translating the shoe at 0.5 m/s and applied a force of 250 N (Iraqi et al., 2018a). A shoe angle of 17 ± 1° was controlled with an adjustable bracket and was verified during testing with a goniometer. These testing methods reflect the

Table 1
List of selected NSR shoes from online vendors. For Gender, the following codes were used based on the manufacturer's description: M: Men's, W: Women's, U: Unisex.

Shoe Code	Online Vendor	Shoe Name	Style	Gender
NSR1	Amazon	New Balance 608-4	Athletic	M
NSR2	Amazon	Asics Gel-Venture 6	Athletic	M
NSR3	Amazon	Brooks Adrenaline GTS 1	Athletic	W
NSR4	ShoeBuy	Skechers D'Lites	Athletic	W
NSR5	Footlocker	Adidas Original Superstar	Comfort	W
NSR6	Macy's	Converse Chuck Taylor	Comfort	W
NSR7	Zappos	Asics Gel Nimbus 20	Athletic	W
NSR8	Amazon	Puma Suede	Comfort	W
NSR9	Amazon	Dockers Gordon Leather	Dress	M
NSR10	Amazon	Clarks Tilden Cap Oxford	Dress	M
NSR11	Zappos	Rockport Margin Oxford	Dress	M
NSR12	ShoeBuy	Keds Champion Leather	Comfort	W
NSR13	Zappos	Vans Old Skool	Comfort	U
NSR14	Zappos	Franco Sarto Bocca	Dress	W
NSR15	Zappos	Dansko	Dress	W

dynamics of slipping and are predictive of human slips (Iraqi et al., 2018a, 2018b). The flooring was attached to a force plate (BERTEC Corporation, Columbus, OH, USA), which sampled at a frequency of 500 Hz. Five trials were collected and the ACOF across these five trials was averaged. The ACOF measurements were collected with an oil contaminant on two flooring materials, ceramic (ASTM, 2016) and laminate (used in (Sundaram et al., 2020)). These surface materials are commonly found in commercial flooring and represent a polymer-based and a clay-based material. In the presence of oily conditions, good correlation has been observed across polymer and clay-based materials (Chanda et al., 2018, 2019). Thus, results from these conditions are expected to be applicable to a wide-range of common flooring materials.

To measure the peak fluid pressure, the floor surface was instrumented with four fluid pressure transducers (Setra, 3100R100PG089, Boxborough, MA, USA). The transducers were placed 25 mm apart. Between each of the five trials, the floor was moved 5 mm with respect to the shoe in the direction transverse to the long axis of the shoe. Overall, this led to 20 scans (4 scans per trial x 5 trials) at 5 mm intervals to capture fluid pressures across the surface of the shoe (Fig. 1). In the direction of shoe sliding, the pressure transducers were placed so that the shoe passed them at half of the slip distance after the target normal force was reached. Fluid pressure was only collected on the laminate flooring because the thickness of the ceramic floor would have led to a substantial gap between the transducer and floor surface. Because fluid pressure is largely sensitive to the shoe features (Hemler et al., 2020; Sundaram et al., 2020), similar trends were expected for ceramic flooring as the laminate flooring. Fluid pressure data were sampled at 500 Hz.

2.3. Collection of NSR shoe parameters

The parameters of tread surface area, hardness, and heel shape were collected since they are known to affect ACOF in SR shoes (Iraqi et al., 2020; Jones et al., 2018). To measure tread surface area, the sole of each NSR shoe was coated with ink and transferred to white paper (Fig. 2). This paper was then scanned and converted to a black and white image (spatial resolution of 0.042 mm). The tread surface area of the heel was measured as the summed black pixel area for the 50 mm most posterior portion of the shoe (Iraqi et al., 2020; Jones et al., 2018). The back 50 mm of the sole was used in this calculation because this area represents the majority of the shoe region where fluid pressures are observed (Singh and Beschorner, 2014).

To measure hardness, a durometer (Shore A durometer based on ASTM standard D2240, 2015) was used. The outsole of the shoe was held flat by a clamp, and a mass of 1 kg was placed on the durometer to improve the accuracy of the hardness readings (Iraqi et al., 2020). The hardness readings were recorded and averaged across five different locations of the 50 mm of the posterior portion of the shoe. The final parameter, heel shape, was classified as either flat or beveled based on observation. Flat shoes were characterized by a heel that touched the floor with no pressure applied. Shoes with a round or chamfer in the sagittal plane were categorized as beveled (Moghaddam and Beschorner, 2017). Beveling was assessed since it has been found to increase ACOF in SR shoes (Iraqi et al., 2020).

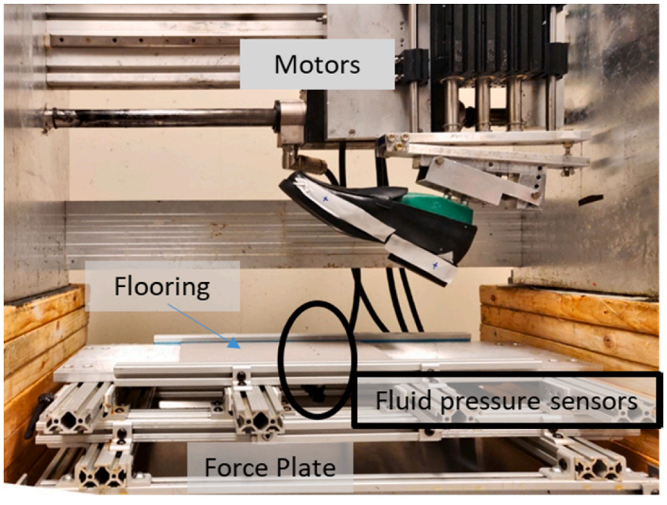

Fig. 1. Portable Slip Tester fitted with the fluid pressure extension (location of pressure sensors shown in oval).

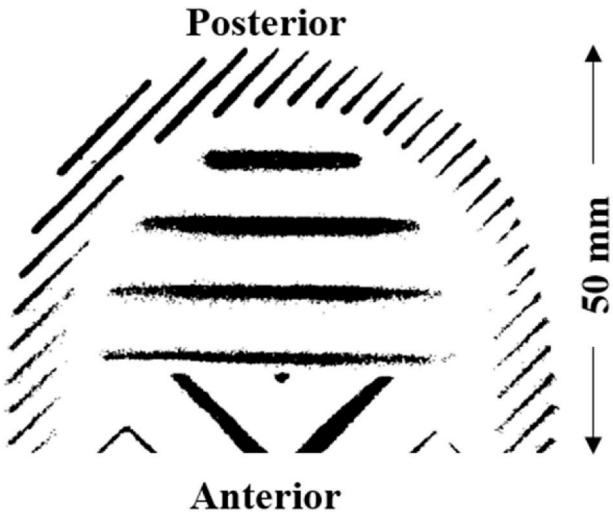

Fig. 2. Scanned ink imprint of a NSR shoe (NSR 6).

2.4. Data and statistical analysis

The ACOF was calculated based on the longitudinal shear force, transverse shear force, and the normal force (see Eq. (1)). These forces were averaged across the 200 ms after the normal force first reached 250 N. The peak fluid pressure was calculated as the maximum value across the four fluid pressure sensors and over the five trials (Beschorner et al., 2020).

$$ACOF = \frac{\sqrt{F^2_{Longitudinal\ Shear} + F^2_{Transverse\ Shear}}}{F_{Normal}} \quad (1)$$

The predicted ACOF was calculated for each of the NSR shoes based on regression equations developed in Iraqi et al. (2020). These regression equations are based on the forward selection model that was deemed to be the preferred model in that study. This model predicts ACOF as a function of tread surface area, heel bevel, hardness, and the flooring (Eq. (2)), where the number in the brackets represents the unit of measure or the dichotomous state of the parameter (e.g., the heel shape variable is 1 for beveled shoes and 0 for non-beveled shoes). The measurement methods for tread parameters and the floor samples were identical in this study to the ones described in Iraqi et al. (2020).

$$ACOF = 0.223 + 0.015 * tread\ surface\ area\ [cm^2] + 0.041 * heel\ shape\ [bevel] - 0.003 * hardness\ [Shore\ A] + 0.254 * floor[ceramic] \quad (2)$$

Statistical analyses were conducted to assess: 1) whether the model previously developed for SR shoes similarly applies to NSR shoes; and 2) to determine whether fluid pressures contribute to friction among NSR shoes (JMP 15.2, Cary, NC, USA). An alpha value of 0.05 was used for all analyses. The research questions presented within this paper were consistent with the planned analyses prior to data collection.

A Wilcoxon signed-rank test was performed to determine if the

measured ACOF values differ significantly from the predicted ACOF based on the model for SR shoes. This method was used because the data was bimodal and trended toward not being normally distributed ($W = 0.94$: $p = 0.070$). The Wilcoxon Signed-Rank Test makes no assumptions about the data distribution and is considered a conservative test since it errors towards controlling Type 1 error for non-normally distributed data. The null hypothesis was that the difference between the actual and predicted friction values was 0 (the predicted values do not systematically overestimate or underestimate ACOF for NSR shoes). The purpose of this analysis was to determine if a bias exists in the ACOF predictions when applied to NSR shoes.

A regression model was created to determine whether the parameters (tread surface area, hardness, and heel shape) that predict ACOF for SR similarly predict ACOF for NSR shoes. The ACOF data for NSR shoes collected in this study were combined with the data previously collected and reported for SR shoes (Iraqi et al., 2020). ACOF was the dependent variable and the independent variables included shoe type (NSR vs. SR), flooring, and the previously observed parameters for predicting friction, specifically tread surface area, hardness, heel shape. First-order interaction effects between the shoe type and each shoe parameter (tread surface area, hardness, and heel shape), and the interaction between shoe type and flooring were also included. After the full model was determined (Eq. (3)), backward elimination step-wise regression was used to remove insignificant parameters from the model, based on the parameter with the largest p-value. These steps were repeated until no parameters in the final model had a p-value greater than 0.05. Shapiro-Wilk W test was applied to assess the distribution of continuous predictors. The distribution of residuals and homoscedasticity were assessed using residual plots. Linearity was also assessed for each regressor.

To test the contribution of fluid drainage to friction performance in NSR shoes, a regression model was applied to determine the effect of peak fluid pressure on the ACOF for NSR shoes. The model regressors included peak fluid pressure, flooring, and their interaction. ACOF was log-transformed to meet the linearity assumption consistent with other papers (Iraqi et al., 2018a). A square root transformation was applied to peak pressure to satisfy the normal distribution assumption, consistent with prior research (Sundaram et al., 2020). This sample size was sufficient for capturing a fluid pressure effect with a Cohen's $f^2 = 0.28$, exceeding the test's sensitivity of prior studies ($f^2 = 0.82$ based on Sundaram et al., 2020). The residuals of the model were assessed with a Shapiro-Wilk Test and residuals were assessed for homoscedasticity. Linearity was also assessed between fluid pressure and ACOF after the transformation was applied.

3. Results

3.1. Descriptive results

The mean ACOF for NSR shoes was 0.119, with a standard deviation of 0.077. The median/mean for peak fluid pressure was 47 kPa/153 kPa, and the interquartile range was 16–295 kPa. Tread surface area had a mean of 8.45 cm^2, with a standard deviation of 4.20 cm^2. Hardness had a mean of 63 with a standard deviation of 11. Finally, 10 NSR shoes were classified as beveled, and 5 had a flat heel shape.

The mean ACOF for SR shoes was 0.394, with a standard deviation of 0.150. Tread surface area had a mean of 11.58 cm^2 with a standard deviation of 2.48 cm^2. SR shoes had an average hardness of 55.42 with a standard deviation of 6.34. Finally, of the 58 SR shoes, 29 were classified as beveled and 29 were classified as flat.

3.2. Does the previously developed ACOF model systematically over or underestimate ACOF in NSR shoes?

The ACOF model systematically overestimated ACOF values of NSR shoes. The median difference was found to differ from 0 ($z = 13.0$, $p < 0.001$). The median of the difference between the estimated and actual ACOF values was 0.19 with an interquartile range of 0.074–0.31. Thus, the magnitude to which this regression model overestimated ACOF for NSR shoes was substantial.

3.3. Linear regression model comparing NSR and SR shoes

After backward stepwise regression was completed, the significant regressors on ACOF were found to be shoe type ($p < 0.0001$, $F_{1,140} = 379.8$), flooring ($p < 0.001$, $F_{1,140} = 155.8$), tread surface area ($p < 0.001$, $F_{1,140} = 23.4$), the interaction between shoe type and flooring ($p < 0.001$, $F_{1,140} = 65.5$), and the interaction between shoe type and tread surface area ($p < 0.0001$, $F_{1,140} = 62.9$). Tread surface area was normally distributed ($W = 0.984$, $p = 0.0858$). The final regression equation is given in Equation (4) ($F_{5,140} = 224.1$). When considering the full data set, the error was relatively low (root mean square error = 0.060), indicating that the regression model fit the data well. Given the significant interaction between the shoe type and tread surface area (Fig. 3), we quantified the sensitivity of SR and NSR shoes to tread surface area. The change in ACOF from the 1st to 3rd quartile in tread surface area led to 0.100 increase in ACOF for SR shoes but a 0.025 reduction in ACOF for NSR shoes. A larger increase in ACOF was observed for the ceramic floor relative to the laminate floor for SR shoes compared with NSR shoes. Thus, the effects of tread surface area and flooring did not generalize across SR and NSR shoes.

Full Model:

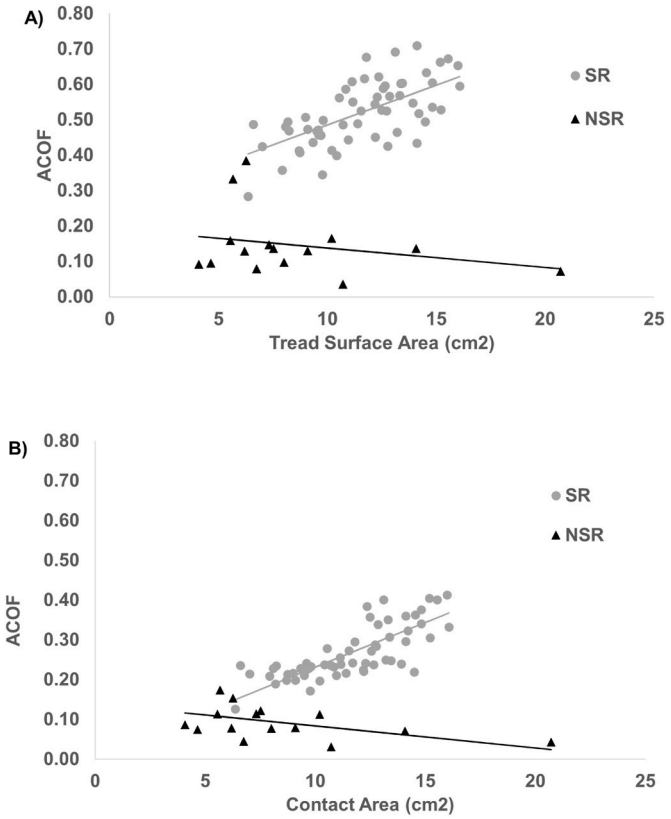

Fig. 3. Response of ACOF to tread surface area for SR (SR, gray circles) and NSR (NSR, black triangle) shoes on ceramic (A) and laminate (B) flooring. The opposite effect of tread surface area for SR and NSR shoes is characterized by the different slope of the SR regression line (gray) from the NSR regression line (black).

$$ACOF = \beta_0 - \alpha_{Shoe\ Type} * Shoe\ Type[NSR] + \alpha_{Heel\ Shape} * Heel\ Shape[Beveled] + \alpha_{Tread\ Surface\ Area} * [Tread\ Surface\ Area] - \alpha_{Hardness} * [Hardness] + \alpha_{Flooring} * [Ceramic] - \alpha_{Shoe\ Type,\ Heel\ Shape} * [Beveled, NSR\ OR\ Flat, SR] - \alpha_{Shoe\ Type,\ Tread\ Surface\ Area} * (Shoe\ Type[NSR] * [Tread\ Surface\ Area]) + \alpha_{Shoe\ Type,\ Hardness} * (Shoe\ Type[NSR] * [Hardness]) + \alpha_{Flooring,\ Shoe\ Type} * (Ceramic, NSR\ OR\ laminate,\ SR) \quad (3)$$

Backward Elimination:

$$ACOF = 0.107 + 0.032 * Shoe\ Type[NSR] + 0.154[Ceramic] + 0.0225[Tread\ Surface\ Area] - 0.028([Tread\ Surface\ Area] * Shoe\ Type\ [NSR]) - 0.0998[NSR,\ ceramic\ OR\ SR,\ laminate] \quad (4)$$

3.4. Linear regression model of peak fluid pressure on ACOF

Flooring ($p = 0.012$, $F_{1,27} = 7.3$) and peak fluid pressure ($p < 0.001$, $F_{1,27} = 20.8$) influenced ACOF for NSR shoes, but not their interaction ($p = 0.85$, $F_{1,26} = 0.0$). Thus, the step-wise method led to the removal of the interaction effect from the final model (Eq. (5)). The residuals were normally distributed ($W = 0.940$, $p = 0.0885$). Increased fluid pressures were associated with a reduction in ACOF (Fig. 4, Eq. (5)). The coefficient of determination (R^2) was 0.51, and the RMS error was 0.064. A 47% decrease in ACOF (0.080 for ceramic and 0.053 for laminate) is predicted as fluid pressure increased from the 1st to 3rd quartile of NSR shoes.

$$ACOF = 0.136 * 1.50[Ceramic] e^{-0.0484 * \sqrt{PeakFluidPressure}} \quad (5)$$

4. Discussion

This study provided clear evidence that regression equations developed for SR shoes based on the assumption of boundary lubrication cannot be applied to NSR shoes. This finding conflicts with the first hypothesis. These models overestimate friction by a large magnitude compared to the observed friction values and the interaction between shoe type and tread surface area indicates that tread surface area has an opposite effect on SR and NSR shoes. The linear regression model showed that the peak fluid pressure and flooring significantly predicted the ACOF for NSR shoes. Thus, the hydrodynamic pressures seem to explain the variability across NSR shoes, while tread design parameters that influence boundary lubrication, as described in Iraqi et al. (2020), seemed to explain the variability for SR shoes. Increasing peak fluid pressure from the 1st to 3rd quartile led to a nearly 50% reduction in ACOF, which indicates that the impact of fluid pressure on NSR shoes was substantial. The first hypothesis that the ACOF of NSR shoes responded similarly to shoe design parameters as SR shoes was rejected. The second hypothesis that the ACOF of NSR shoes was dependent on under-shoe fluid pressures was confirmed.

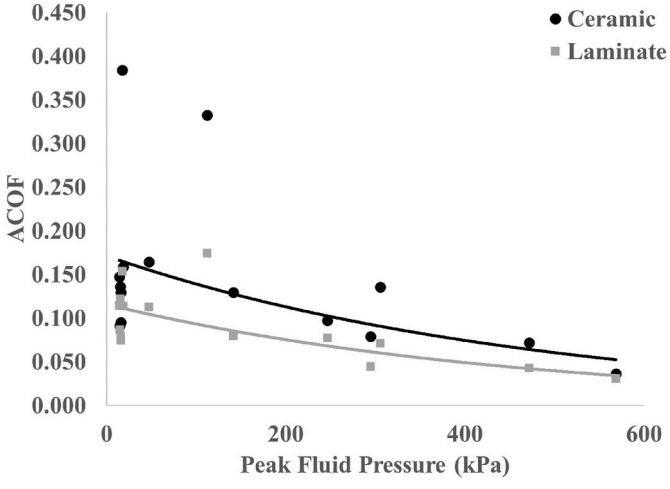

Fig. 4. Linear Regression model of ACOF predicted by the peak fluid pressure and flooring. The fit lines are not linear due to the transformations (ln(*ACOF*), $\sqrt{Peak\ Fluid\ Pressure}$) that were performed. The overall regression equation is seen in Equation (5).

The high fluid pressures that were observed for NSR shoes indicate that the tread channels were insufficient for fluid drainage. This result is consistent with previous research that showed higher fluid pressures for worn NSR shoes compared to worn SR shoes (Sundaram et al., 2020). The negative slope that was observed between ACOF and fluid pressure is consistent with previous research, which suggests that the separation of the floor and shoe due to a fluid contaminant pressurization reduces the ACOF substantially (Beschorner and Singh, 2012). Thus, this research adds to the growing body of evidence that under-shoe fluid pressurization is a relevant factor for shoe friction performance and the risk of slipping. Finally, the poor friction performance associated with popular shoes (Fig. 3) is consistent with finding based on icy friction performance (Bagheri et al., 2019b, 2019c).

Clearly, the impact of tread surface area and flooring on ACOF for NSR shoes was inconsistent with previous research that measured its impact on ACOF for SR shoes (Iraqi et al., 2020; Jones et al., 2018). One explanation for this discrepancy is that different mechanisms were dominating the variability in friction between these two shoe types. Boundary lubrication, which has been shown to apply to SR shoes, describes the condition in which the liquid film between the shoe and floor is not pressurized (F.Sadeghi, 2010). For SR shoes, boundary lubrication is promoted by tread channels that provide a low-resistance means for the fluid to escape from the under-shoe interface (Beschorner et al., 2014; Hemler et al., 2020). However, based on the results of the collected fluid pressure values in this study, the tread pattern of NSR shoes does not allow for the fluid to drain causing the shoe to operate in mixed or hydrodynamic lubrication. This finding may explain why increasing tread surface area for NSR shoes without increasing channels for fluid escape results in a decrease in ACOF. The larger continuous contact regions of the NSR shoes may have mimicked worn regions (Walter et al., 2021), which lead to a reduction in ACOF as their size (and surface area) increases (Hemler et al., 2019, 2020; Sundaram et al., 2020). Interestingly, the flooring had a larger effect on ACOF for SR shoes than NSR shoes consistent with prior research (Beschorner et al., 2017). Floor roughness has a large impact on hysteresis friction when the shoe is operating in boundary lubrication (Cowap et al., 2015; Moghaddam et al., 2015). Thus, SR shoes operating in boundary lubrication, may be able to realize the benefits of high roughness flooring more than NSR shoes that are operating in mixed lubrication.

The key finding is that the set of diagnostic methods used to improve friction for SR shoes do not apply to NSR shoes. Thus, a different set of tools is needed that focuses on reducing fluid pressures such that shoes operate closer to boundary lubrication. One possibility would be to test whether NSR shoe treads can be modeled using a tapered wedge model that was recently validated for worn SR shoes (Hemler et al., 2020).

Other factors beyond tread drainage may also be relevant like the surface energy of the shoe materials and their porosity (Yamaguchi et al., 2018). Thus, further research is needed to develop dedicated prediction models for NSR shoes.

Certain limitations pertaining to generalizability and this study's methodology should be acknowledged. As this testing only included fifteen NSR shoes, the regression model connecting fluid pressures to ACOF may not have been trained with sufficient data to be precise. While the 15 selected shoes represent some of the most popular shoe products at the time of purchase, they only represent a small fraction of the overall shoe products available. Improved friction performance may be observed in certain categories of NSR shoes (e.g., hiking boots).

This paper has shown that the model to predict ACOF for SR shoes cannot be applied to NSR shoes. As a result of these differences, tread surface area has an opposite effect for the two shoe types, and the effect of flooring on ACOF is smaller for NSR shoes. Furthermore, this study has shown that there is at least one extra parameter, peak fluid pressure, that needs to be acccounted for in a prediction model for ACOF of NSR shoes. This indicates that designers of NSR shoes should prioritize tread drainage channels when attempting to improve the friction performance of their shoes.

Declaration of competing interest

The authors do not have any other competing interests to declare.

Acknowledgements

Funding: This study was supported by the National Institute for Occupational Safety & Health (R03 OH011069).

References

Aschan, C., Hirvonen, M., Mannelin, T., Rajamaki, E., 2005. Development and validation of a novel portable slip simulator. Appl. Ergon. 36, 585–593.
ASTM, 2016. ASTM F2508-16e1: Standard Practice for Validation, Calibration, and Certification of Walkway Tribometers Using Reference Surfaces. ASTM International, West Conshohocken, PA.
Bagheri, Z.S., Anwer, A.O., Fernie, G., Naguib, H.E., Dutta, T., 2019a. Effects of multi-functional surface-texturing on the ice friction and abrasion characteristics of hybrid composite materials for footwear. Wear 418, 253–264.
Bagheri, Z.S., Patel, N., Li, Y., Morrone, K., Fernie, G., Dutta, T., 2019b. Slip resistance and wearability of safety footwear used on icy surfaces for outdoor municipal workers. Work 62, 37–47.
Bagheri, Z.S., Patel, N., Li, Y., Rizzi, K., Lui, K.Y.G., Holyoke, P., Fernie, G., Dutta, T., 2019c. Selecting slip resistant winter footwear for personal support workers. Work 64, 135–151.
Bagheri, Z.S., Beltran, J.D., Holyoke, P., Dutta, T., 2021. Reducing fall risk for home care workers with slip resistant winter footwear. Appl. Ergon. 90, 103230.
Beschorner, K.E., Singh, G., 2012. A Novel Method for Evaluating the Effectiveness of Shoe-Tread Designs Relevant to Slip and Fall Accidents. Human Factors and Ergonomics Society, Boston, MA.
Beschorner, K.E., Albert, D.A., Chambers, A.J., Redfern, M.R., 2014. Fluid pressures at the shoe-floor-contaminant interface during slips: effects of tread & implications on slip severity. J. Biomech. 47, 458–463.
Beschorner, K.E., Jones, T.G., Iraqi, A., 2017. The Combined Benefits of Slip-Resistant Shoes and High Traction Flooring on Coefficient of Friction Exceeds Their Individual Contributions. Proceedings of the Human Factors and Ergonomics Society Annual Meeting. SAGE Publications Sage CA: Los Angeles, CA, pp. 931–935.
Beschorner, K.E., Siegel, J.L., Hemler, S.L., Sundaram, V.H., Chanda, A., Iraqi, A., Haight, J.M., Redfern, M.S., 2020. An observational ergonomic tool for assessing the worn condition of slip-resistant shoes. Appl. Ergon. 88, 103140.
Blanchette, M.G., Powers, C.M., 2015. The influence of footwear tread groove parameters on available friction. Appl. Ergon. 50, 237–241.
Bureau of Labor Statistics, 2020. TABLE R31. Number of nonfatal occupational injuries and illnesses involving days away from work by event or exposure leading to injury or illness and selected natures of injury or illness. private industry, 2019. In: U.S. Department of Labor (Ed.), Washington, D.C.
Burnfield, J.M., Powers, C.M., 2006. Prediction of slips: an evaluation of utilized coefficient of friction and available slip resistance. Ergonomics 49, 982–995.
Chanda, A., Jones, T.G., Beschorner, K.E., 2018. Generalizability of footwear traction performance across flooring and contaminant conditions. In: IISE Transactions on Occupational Ergonomics and Human Factors, 6, pp. 98–108.
Chanda, A., Reuter, A., Beschorner, K.E., 2019. Vinyl composite tile surrogate for mechanical slip testing. In: IISE Transactions on Occupational Ergonomics and Human Factors, pp. 1–10.
Chang, W.-R., 1998. The effect of surface roughness on dynamic friction between neolite and quarry tile. Saf. Sci. 29, 89–105.
Chang, W.-R., Kim, I.-J., Manning, D.P., Bunterngchit, Y., 2001a. The role of surface roughness in the measurement of slipperiness. Ergonomics 44, 1200–1216.
Chang, W.R., Gronqvist, R., Leclercq, S., Myung, R., Makkonen, L., Strandberg, L., Brungraber, R.J., Mattke, U., Thorpe, S.C., 2001b. The role of friction in the measurement of slipperiness, Part 1: friction mechanisms and definition of test conditions. Ergonomics 44, 1217–1232.
Chang, W.-R., Grönqvist, R., Hirvonen, M., Matz, S., 2004. The effect of surface waviness on friction between Neolite and quarry tiles. Ergonomics 47, 890–906.
Chen, C.-C., Chen, Z.-X., Chang, C.-L., Lin, F.-L., 2015. The slip-resistance effect evaluation of floor roughness under different liquid viscosity. Procedia Manufacturing 3, 5007–5013.
Courtney, T.K., Sorock, G.S., Manning, D.P., Collins, J.W., Holbein-Jenny, M.A., 2001. Occupational slip, trip, and fall-related injuries–can the contribution of slipperiness be isolated? Ergonomics 44, 1118–1137.
Cowap, M., Moghaddam, S., Menezes, P., Beschorner, K., 2015. Contributions of adhesion and hysteresis to coefficient of friction between shoe and floor surfaces: effects of floor roughness and sliding speed. Tribol. Mater. Surface Interfac. 9, 77–84.
Florence, C., Haegerich, T., Simon, T., Zhou, C., Luo, F., 2015. Estimated lifetime medical and work-loss costs of emergency department–treated nonfatal injuries — United States, 2013. MMWR (Morb. Mortal. Wkly. Rep.) 64, 1078–1082.
Grönqvist, R., 1995. Mechanisms of friction and assessment of slip resistance of new and used footwear soles on contaminated floors. Ergonomics 28, 224–241.
Hale, J., O'Connell, A., Lewis, R., Carré, M., Rongong, J., 2021. An evaluation of shoe tread parameters using FEM. Tribol. Int. 153, 106570.
Hamrock, B.J., Schmid, S.R., Jacobson, B.O., 2004. Fundamentals of Fluid Film Lubrication. Marcel Dekker Inc., New York.
Hanson, J.P., Redfern, M.S., Mazumdar, M., 1999. Predicting slips and falls considering required and available friction. Ergonomics 42, 1619–1633.
Hemler, S., Charbonneau, D., Iraqi, A., Redfern, M.S., Haight, J.M., Moyer, B.E., Beschorner, K.E., 2019. Changes in under-shoe traction and fluid drainage for progressively worn shoe tread. Appl. Ergon. 80, 35–42.
Hemler, S., Charbonneau, D., Beschorner, K., 2020. Predicting hydrodynamic conditions under worn shoes using the tapered-wedge solution of Reynolds equation. Tribol. Int. 145, 106161.
Iraqi, A., 2013. Comparison of Interfacial Fluid Pressures Generated across Common Shoe-Floor Friction Testing Apparatuses. Department of Mechanical Engineering. Blekinge Institute of Technology, Karlskrona, Sweden.
Iraqi, A., Cham, R., Redfern, M.S., Beschorner, K.E., 2018a. Coefficient of friction testing parameters influence the prediction of human slips. Appl. Ergon. 70, 118–126.
Iraqi, A., Cham, R., Redfern, M.S., Vidic, N.S., Beschorner, K.E., 2018b. Kinematics and kinetics of the shoe during human slips. J. Biomech. 74, 57–63.
Iraqi, A., Vidic, N.S., Redfern, M.S., Beschorner, K.E., 2020. Prediction of coefficient of friction based on footwear outsole features. Appl. Ergon. 82, 102963.
Jones, T.G., Iraqi, A., Beschorner, K.E., 2018. Performance testing of work shoes labeled as slip resistant. Appl. Ergon. 68, 304–312.
Kubis, P., Randesi, J., 2013. Slip-resistant Footwear Tread. Google Patents.
Li, K.W., Chen, C.J., 2004. The effect of shoe soling tread groove width on the coefficient of friction with different sole materials, floors, and contaminants. Appl. Ergon. 35, 499–507.
Li, K.W., Chen, C.J., 2005. Effects of tread groove orientation and width of the footwear pads on measured friction coefficients. Saf. Sci. 43, 391–405.
Moghaddam, S., Beschorner, K., 2017. Sensitivity of a Multiscale Model of Shoe-Floor-Contaminant Friction to Normal Force and Shoe-Floor Contact Angle, 2017. STLE Annual Meeting & Exhibition.
Moghaddam, S.R.M., Beschorner, K.E., 2018. Predicting shoe-floor contact pressures and their impact on coefficient of friction using finite element analysis. Tribol. Lubric. Technol. 74, 26–28.
Moghaddam, S.R.M., Redfern, M.S., Beschorner, K.E., 2015. A microscopic finite element model of shoe–floor hysteresis and adhesion friction. Tribol. Lett. 59, 1–10.
Moghaddam, S.R., Acharya, A., Redfern, M.S., Beschorner, K.E., 2018. Predictive multiscale computational model of shoe-floor coefficient of friction. J. Biomech. 66, 145–152.
Moore, C.T., Menezes, P.L., Lovell, M.R., Beschorner, K.E., 2012. Analysis of shoe friction during sliding against floor material: role of fluid contaminant. J. Tribol. 134, 041104.
National Center for Injury Prevention and Control, 2020. 10 leading causes of nonfatal injuries, United States: 2019, all races , both sexes , disposition: all cases. In: Control, C.f.D (Ed.), Atlanta, GA.
Persson, B.N., 2001. Theory of rubber friction and contact mechanics. J. Chem. Phys. 115, 3840–3861.
Rizvi, R., Naguib, H., Fernie, G., Dutta, T., 2015. High friction on ice provided by elastomeric fiber composites with textured surfaces. Appl. Phys. Lett. 106, 111601.
Roshan Fekr, A., Li, Y., Gauvin, C., Wong, G., Cheng, W., Fernie, G., Dutta, T., 2021. Evaluation of winter footwear: comparison of test methods to determine footwear slip resistance on ice surfaces. Int. J. Environ. Res. Publ. Health 18, 405.
Sadeghi, F., 2010. Elastohydrodynamic lubrication. In: Rahnejat, H. (Ed.), Tribology and Dynamics of Engine and Powertrain. Woodhead Publishing, pp. 171–221.
Schaefer, S., Lindenberger, U., 2013. Thinking while walking: experienced high-heel walkers flexibly adjust their gait. Front. Psychol. 4, 316.
Singh, G., Beschorner, K.E., 2014. A method for measuring fluid pressures in the shoe–floor–fluid interface: application to shoe tread evaluation. In: IIE Transactions on Occupational Ergonomics and Human Factors, 2, pp. 53–59.
Strandberg, L., 1985. The effect of conditions underfoot on falling and overexertion accidents. Ergonomics 28, 131–147.

Strobel, C.M., Menezes, P.L., Lovell, M.R., Beschorner, K.E., 2012. Analysis of the contribution of adhesion and hysteresis to shoe–floor lubricated friction in the boundary lubrication regime. Tribol. Lett. 47, 341–347.
Sundaram, V., Hemler, S.L., Chanda, A., Haight, J.M., Redfern, M.S., Beschorner, K.E., 2020. Worn region size of shoe soles impacts human slips: testing a mechanistic model. J. Biomech. 109797.
Tisserand, M., 1985. Progress in the prevention of falls caused by slipping. Ergonomics 28, 1027–1042.
U.S. Department of Labor- Bureau of Labor Statistics, 2020. Nonfatal Cases Involving Days Away from Work: Selected Characteristics (2011 Forward) Series ID: CSU00X42XXXX6E000. CSU00X422XXX6E000. Washington, D.C.
Verma, S.K., Chang, W.R., Courtney, T.K., Lombardi, D.A., Huang, Y.-H., Brennan, M.J., Mittleman, M.A., Ware, J.H., Perry, M.J., 2011. A prospective study of floor surface, shoes, floor cleaning and slipping in US limited-service restaurant workers. Occup. Environ. Med. 68, 279–285.
Walter, P.J., Tushak, C.M., Hemler, S.L., Beschorner, K.E., 2021. Effect of tread design and hardness on interfacial fluid force and friction in artificially worn shoes. In: Footwear Science in review.
Yamaguchi, T., Katsurashima, Y., Hokkirigawa, K., 2017. Effect of rubber block height and orientation on the coefficients of friction against smooth steel surface lubricated with glycerol solution. Tribol. Int. 110, 96–102.
Yamaguchi, T., Sugawara, T., Takahashi, M., Shibata, K., Moriyasu, K., Nishiwaki, T., Hokkirigawa, K., 2018. Effect of porosity and normal load on dry sliding friction of polymer foam blocks. Tribol. Lett. 66, 1–9.